

Predicting Respiratory Anomalies and Diseases Using Deep Learning Models

Lam Pham¹

Abstract—In this paper, robust deep learning frameworks are introduced, aims to detect respiratory diseases from respiratory sound inputs. The entire processes firstly begins with a front-end feature extraction that transforms recordings into spectrograms. Next, a back-end deep learning model classifies the spectrogram features into categories of respiratory disease or anomaly. Experiments are conducted over the ICBHI benchmark dataset of respiratory sounds. According to obtained experimental results, we make three main contributions toward lung-sound analysis: Firstly, we provide an extensive analysis on common factors (type of spectrogram, time resolution, cycle length, or data augmentation, etc.) that affect final prediction accuracy in a deep learning based system. Secondly, we propose novel deep learning based frameworks by using the most influencing factors indicated. As a result, the proposed deep learning frameworks outperforms state of the art methods. Finally, we successfully to apply the Teacher-Student scheme to solve the trade-off between model performance and model size that helps to increase ability of building real-time applications.

Clinical relevance— Respiratory disease, wheezes, crackles, anomaly detection, Convolutional Neural Network (CNN), Recurrent Neural Network (RNN), mixup data augmentation, Mixture of Expert (MoE), Gammatone spectrogram.

I. INTRODUCTION

According to an analysis conducted by the World Health Organization [1], it is fact that respiratory illness, which comprises of lung cancer, tuberculosis, asthma, chronic obstructive pulmonary disease (COPD), and lower respiratory tract infection (LRTI), account for a high percentage of mortality worldwide. Indeed, annual record indicates around 10, 65 and 334 million people currently suffering from tuberculosis (TB), chronic obstructive pulmonary disease (COPD), and asthma, respectively. Noticeably, there are about 1.4, 1.6, and 3 million people die by TB, lung cancers, and COPD each year. To deal with respiratory diseases, early detection is the key factor to increase effectiveness of treatment as well as limit spread. In an respiratory examination, lung auscultation is an important part to diagnose respiratory diseases. By listening to the sounds produced during lung auscultation, experts can recognize adventitious sounds (e.g., *Crackles* and *wheezes*) in the respiratory cycle that usually occurs in people suffering pulmonary disorders. If automated methods can be developed to detect these anomaly sounds, it may be useful in enhancing the early detection of respiratory disease in future. Although automated analysis of respiratory sounds were early conducted [2], [3], [4], the research field attracted little attention. However, it has drawn much attention in

recent years due to applying robust machine learning and deep learning techniques.

As regards machine learning approach, proposed systems used for respiratory sound analysis tend to rely upon frame-based representations. Most researches [5], [6] approached Frequency Cepstral Coefficients (MFCC), the most popular feature used in Automatic Speech Recognition (ASR) research field, to derive feature vectors. Using both spectral and temporal features, Melby et al. [7] extracted five-dimensional feature vectors from draw audio signal, comprising of four features from the time domain (variance, range, and sum of simple moving average, sum of simple moving average) and one feature from the frequency domain (spectrum mean). Meanwhile, Hanna et al. [8] firstly extracted spectral information from barkbands, energybands, melbands, mfcc, etc. , the rythm features from beats loudness, bpm, etc), the harmonicity and inharmonicity features, and the tonal features (chords strength, tuning frequency, etc). Next, they computed statistical values such as standard deviation, variance, minimum and maximum, median, mean, means of first and second derivatives and variances of first and second derivatives from the features to maximize the chance of correct feature representation. To further explore audio features, Mendes et al. [9] proposed to use 35 different types of features, mainly come from the research of Music Information Retrieval. Inspire that only some certain features mainly affect the final result, Datta et al. [10] firstly extracted various features such as power spectral density (PSD), FFT and Wavelet spectrogram, Frequency Cepstral Coefficients (MFCC), and Linear Frequency Cepstral Coefficients (LFCC). Next, they applied a Maximal Information Coefficient (MIC) [11] to score these features, thus selected the the most influencing features before feeding into a classifier. Similarly, Kok et al. [6] applied the Wilcoxon Sum of Rank test to indicate which feature among MFCC, Discrete Wavelet Transform (DWT) and Time Domain Features (the power, mean, variance, skewness and kurtosis of audio signal) mainly affect the final accuracy. Approach image processing techniques, Sengupta et al. [12] applied Local Binary Pattern (LBP) analysis on mel-frequency spectral coefficient (MFSC) spectrogram to capture texture information of the spectrogram. Next, LBP spectrogram is converted into Histogram presentation before feeding into a back-end classification. Ordinarily, frame-based features, likely vectors, are classified by traditional machine learning models such as Logistic Regression [9], K-Nearest Neighbor (KNN) [7], [12], Hidden Markov Model [5], [13], Support Vector Machine [7], [10], [12], [14] or decision trees [6],

¹L. Pham is with the University of Kent, School of Computing, Medway, Kent, UK.

[7], [8].

Regarding deep learning techniques achieved strong and robust detection performance for general sounds [15], [16], feature extraction involves generating two-dimensional spectrograms that is able to capture both temporal and spectral information and present much wider time context than single frame analysis. While there are a variety of spectrogram transformations, Mel-based methods such as log-Mel [17], [18], [19] and MFCC [20], [17], [21], [22], [23], [24] are the most popular approach. Some papers approached different spectrograms such as a combination of two spectrograms (STFT and Wavelet) proposed by Minami et al. [25], optimized S-Transformation in [26]. Current deep learning classifiers exploring spectrogram representation of respiratory sounds mainly base on Convolutional Neural Network (CNN), Recurrent Neural Network (RNN), or hybrid architectures. As regard CNN-based network, published papers presented diverse architectures such as Lenet6 [21], [20], VGG5 [18], two parallel VGG16 [25], and Resnet50 [26]. Inspire that adventitious respiratory sounds such as *Crackle* and *Wheeze* present certain temporal sequence and RNN-based networks able to capture these structures, Perna and Tagarelli [22] conducted a comprehensive analysis of using Long Short-term Memory (LSTM) network, which is used for both tasks of classifying anomaly respiratory sounds and respiratory diseases. By using both LSTM and Gated Recurrent Unit (GRU) cells, learning components in a RNN-based network, Kochetov et al. [24] proposed a novel architecture, namely Noise Masking Recurrent Neural Network, which aims to distinguish both noise and anomaly respiratory sounds. As regards hybrid architectures proposed in [19], [25], CNN is firstly used to map spectrogram input to a time sequence. Next, LSTM [19] or GRU [25] cells are used to learn structure of the sequence before sending to fully-connected layers for final classification.

Compare with machine learning approach, state-of-the-art comparison presented in [22], [26] indicates that deep learning classifiers are more robust and effective to achieve good scores. However, deep learning based models show much more complicated architecture, thus require a large memory when large models are integrated into wearable devices or certain embedded systems for real-time applications. In other words, the state-of-the-art systems present a trade-off between model performance and model size. Additionally, although recent deep learning techniques help to achieve good performance in terms of classification of respiratory sounds, it is hard to compare systems due to the use of different datasets, mainly collected by authors, and often not publicly available.

In this paper, we propose robust deep learning frameworks evaluated on ICBHI dataset [27], aim to

- Compare our results to the state-of-the-art systems due to using the published ICBHI dataset. Furthermore, as ICBHI is one of the biggest datasets of respiratory sounds currently, it is beneficial to make proposed deep learning models general.
- Provide a comprehensive analysis of various fac-

tors, such as type of spectrogram, overlap/non-overlap patches and patch size, data augmentation, etc., thus propose two best deep learning models, each targets individual task of either anomaly respiratory sound classification or respiratory disease detection.

- Solve the trade-off between model performance and model size by applying Student-Teacher scheme. In particular, we consider the best deep learning model as Teacher. We extract middle layers' information from Teacher model and consider the values as soft labels. Next, we use the soft labels to train another model, called Student, with smaller size. Eventually, we obtain the small-size model (Student network trained with soft labels), showing similar performance to Teacher model.

II. ICBHI DATASET AND OUR TASKS PROPOSED

A. ICBHI dataset

The 2017 Internal Conference on Biomedical Health Informatics (ICBHI) [27] provided a large dataset of respiratory sounds. Particularly, it comprises of 920 audio recordings over 5.5 hours. The audio recordings have various lengths from 10 to 90s, recorded with a wide range of sampling frequencies from 4kHz to 44.1kHz. ICBHI dataset was collected from a total of 128 patients, thus identified their situation in terms of being healthy or exhibiting one of the following respiratory diseases or conditions (COPD, Bronchiectasis, Asthma, Upper and Lower respiratory tract infection, Pneumonia, Bronchiolitis) and labelled diseases' name on each audio recording. Inside each audio recording, different types of respiratory cycle, called *Crackle*, *Wheeze*, *Crackle & Wheeze*, and *Normal*, are presented. These cycles were labelled by experts, thus provide onset and offset time. Noticeably, these cycles have various recording lengths (from 0.2s up to 16.2s), with the number of cycles being unbalanced (1864, 886, 506 and 3642 cycles respectively for *Crackle*, *Wheeze*, *Crackle & Wheeze*, and *Normal*).

B. Main tasks from ICBHI dataset

Given this metadata, the ICBHI challenge is separated into two main tasks. Task 1, referred to as respiratory anomaly classification, is separated into two sub-tasks. The first sub-task aims to classify four different cycles (*Crackle*, *Wheeze*, *Crackle & Wheeze*, and *Normal*). The second sub-task is for classifying four types of cycles into two groups of *Normal* and *Anomaly* cycles (the latter consisting of *Crackle*, *Wheeze*, *Both Crackle & Wheeze*). We named these tasks as Task 1-1 and Task 1-2.

Task 2, referred to as respiratory disease prediction, also comprises two sub-tasks. The first sub-task aims to classify audio recordings into groups of disease conditions: *Healthy*, *Chronic Disease* (i.e. COPD, Bronchiectasis and Asthma) and *Non-Chronic Disease* (i.e. Upper and Lower respiratory tract infection, Pneumonia, and Bronchiolitis). The second sub-task is for two groups of *healthy* or *unhealthy* (i.e. the *chronic* and *non-chronic* disease groups combined). We named these tasks as Task 2-1 and Task 2-2. While Task

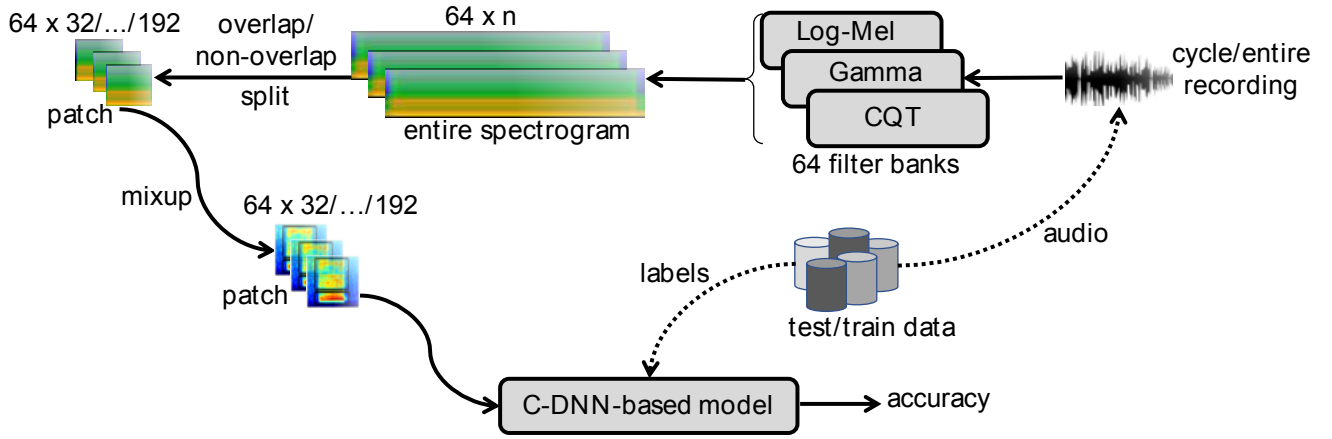


Fig. 1. High-level system architecture

1-1 and 1-2 are evaluated over respiratory cycles, Task 2-1 and 2-2 are evaluated over entire audio recordings.

C. Evaluation metric and our setting

In this paper, we attempt all of the ICBHI challenge tasks recently mentioned. To evaluate our systems over each task, we separate the ICBHI dataset (6898 respiratory cycles for Task 1-1, Task 1-2 and 920 entire recordings for Task 2-1 and Task 2-2) into five-folds for cross validation. We firstly introduce a baseline system, thus conduct experiments on the baseline to indicate the most influencing factors over just the first fold. From the analysis of such factors, we propose the best system configurations and evaluate over all folds. Noting that we eventually propose two deep learning framework, each for individual task of either anomaly cycle detection (Task 1-1 and 1-2) or respiratory disease detection (Task 2-1 and 2-2). To evaluate proposed system and compare to the state of the art, we follow the ICBHI criteria and settings, and report results in terms of sensitivity, specificity and ICBHI score as defined in [27], [22] below,

$$Sensitivity = \frac{C_{crackles} + C_{wheezes} + C_{both}}{N_{crackles} + N_{wheezes} + N_{both}} \quad (1)$$

for classifying four classes of cycles in Task 1-1,

$$Sensitivity = \frac{C_{crackle-or-wheeze}}{N_{crackle-or-wheeze}} \quad (2)$$

for two groups of normal or adventitious cycle in Task 1-2, and

$$Specificity = \frac{C_{normal}}{N_{normal}} \quad (3)$$

where $C_{...}$ and $N_{...}$ are the number of correct inference and the total cases. Similarly, respiratory-disease classification in Task 2-1 and 2-2 provides criteria as below equations.

$$Sensitivity = \frac{C_{chronic} + C_{non-chronic}}{N_{chronic} + N_{non-chronic}} \quad (4)$$

for three groups of diseases in Task 2-1,

$$Sensitivity = \frac{C_{chronic-or-nonchronic}}{N_{chronic-or-nonchronic}} \quad (5)$$

for two groups of healthy or unhealthy in Task 2-2, and

$$Specificity = \frac{C_{healthy}}{N_{healthy}} \quad (6)$$

where $C_{...}$ and $N_{...}$ are the number of correct inference and the total cases. The ICBHI score is computed by averaging of *Sensitivity* and *Specificity*.

III. HIGH-LEVEL SYSTEM AND THE BASELINE ARCHITECTURE PROPOSED

A. High-level system architecture

Firstly, high-level system architecture used for all tasks of anomaly sounds and disease detection is introduced as described in Figure 1. As Figure 1 shown, the entire system is separated into two main steps, comprising a front-end feature extraction (the upper part) and a back-end deep learning models (the lower part). Particularly, cycles in Tasks 1 or entire audio recording in Tasks 2 are transformed into spectrogram representation. The entire spectrogram is thus split into image patches. Next, mixup data augmentation is applied on image patches to generate new data before feeding into deep learning models for classification.

B. Baseline architecture proposed

From the high-level system architecture in Figure 1, it can be seen that there are a variety of factors affecting deep-learning-based system's performance such as cycle length (only for Task 1-1 and 1-2), type of spectrogram, overlap or non-overlap splitting, patch size, data augmentation. It is fact that non of research on respiratory sounds has analysed all these factors. We, therefore, provide an intensive analysis, thus indicate the most influencing factors in this paper. To do this, we firstly introduce a baseline system architecture with setting shown in Table I. By only selecting one option of each factor, we firstly re-sample all audio recoding to 16kHz due to different sample rates. Since cycle lengths are different, we duplicate short respiratory cycles to ensure input features have a minimum length (e.g. 5 s or longer – this is unnecessary for Task 2 which uses entire recordings).

TABLE I
BASELINE SYSTEM SETTING PROPOSED.

Factors	Setting
Re-sample	16KHz
Cycle duration (only for Task 1)	5s
Spectrogram	log-Mel
Patch Splitting	non-overlap
Patch size	64 × 64
Data augmentation	None
Deep learning model	C-DNN based architecture

Next, each cycle or recording audio is then transformed into a log-Mel spectrogram with window size=1024 samples, hop size=256, FFT length=2048 and filter number=64. The resulting spectrogram is then non-overlap split into smaller patches of 64×64. As data augmentation is one of factors evaluated, we do not apply this technique on the baseline system. As regards deep learning model used for the baseline system, we propose a **C-DNN** network architecture, likely VGG-7, as shown in Table II. The **C-DNN** contains 7 sub-blocks, comprising 6 Conv. Blocks and 1 Dense Block, which perform batch normalization (Bn), convolution (Cv[kernel size]), rectified linear units (Relu), average pooling (Ap[kernel size]), global average pooling (Gap), drop out (Dr (percentage drop)), Fully-connected (Fl) and final Softmax layer for classification. C is the number of categories classified that depends on specific tasks. In particular, we use two **C-DNN** models, each set textitC to 3 and 4 for Task 1-1, 1-2 and Task 2-1, 2-2, respectively. Note that as each model is used for each Task, obtained parameters of each model are different after training.

TABLE II

C-DNN NETWORK ARCHITECTURE USED IN THE BASELINE SYSTEM

Architecture	layers	Output
Input layer	Input layer (image patch)	64×64
Conv. Block 01	Bn - Cv [3×3] - Relu - Bn - Ap [2×2] - Dr (10%)	32×32×64
Conv. Block 02	Bn - Cv [3×3] - Relu - Bn - Ap [2×2] - Dr (15%)	16×16×128
Conv. Block 03	Bn - Cv [3×3] - Relu - Bn - Dr (20%)	16×16×256
Conv. Block 04	Bn - Cv [3×3] - Relu - Bn - Ap [2×2] - Dr (20%)	8×8×256
Conv. Block 05	Bn - Cv [3×3] - Relu - Bn - Dr (25%)	8×8×512
Conv. Block 06	Bn - Cv [3×3] - Relu - Bn - Gap - Dr (25%)	512
Dense Block	Fl - Softmax layer	C

C. Experimental setting of the baseline system

We use TensorFlow framework to build **C-DNN** models with hyperparameters set to Adam optimiser [28], 100 epoches, batch size of 100, and cross-entropy loss as below,

$$Loss_{Entropy}(\theta) = -\frac{1}{N} \sum_{i=1}^N \mathbf{y}_i \cdot \log \{\hat{\mathbf{y}}_i(\theta)\} + \frac{\lambda}{2} \cdot \|\theta\|_2^2 \quad (7)$$

where θ is all trainable parameters, N is batch size, and constant λ set initially to 0.0001. \mathbf{y}_i and $\hat{\mathbf{y}}_i$ denote expected and predicted results.

As an entire spectrogram or cycle is separated into patches and applied patch-by-patch to the C-DNN model which then returns the posterior probability computed over each patch. The posterior probability of an entire spectrogram can then be computed by taking the average of all patches' posterior

probabilities. Let us consider $\mathbf{P}^n = (\mathbf{p}_1^n, \mathbf{p}_2^n, \dots, \mathbf{p}_C^n)$, with C being the category number and the n^{th} out of N patches fed into learning model, as the probability of a test sound instance, then the mean classification probability is denoted as $\bar{p} = (\bar{p}_1, \bar{p}_2, \dots, \bar{p}_C)$ where,

$$\bar{p}_c = \frac{1}{N} \sum_{n=1}^N \mathbf{p}_c^n \quad for \quad 1 \leq n \leq N \quad (8)$$

and the predicted label \hat{y} from the C-DNN is determined using,

$$\hat{y} = \operatorname{argmax}(\bar{p}_1, \bar{p}_2, \dots, \bar{p}_C) \quad (9)$$

IV. ANALYSE INFLUENCING FACTORS

By using the baseline system recently proposed, we conduct experiments to evaluate effect of factors mentioned, thus propose the best options of these factors in this Section.

A. Spectrogram analysis

As our previous work's results on sound scene DCASE dataset [29], [30], spectrogram is one of the most important factors affect the final classification. Therefore, effect of spectrogram factor on the baseline is firstly evaluated on all tasks. In particular, baseline system's setting as described in Table I is remained, but type of spectrogram is replaced by log-Mel [31], Gammatone filter (Gamma.) [32], Mel-Frequency Cepstral Coefficient (MFCC) [31], and Constant Q Transform (CQT) [31] in the order. The obtained results

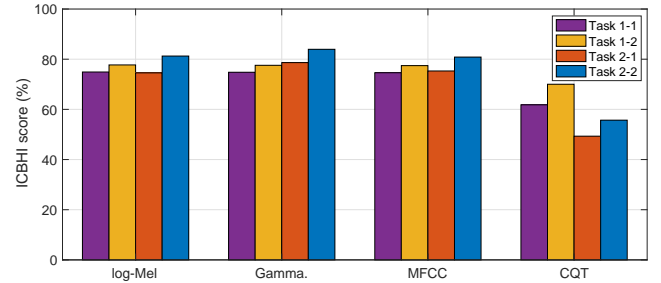


Fig. 2. Baseline performance comparison with different spectrograms

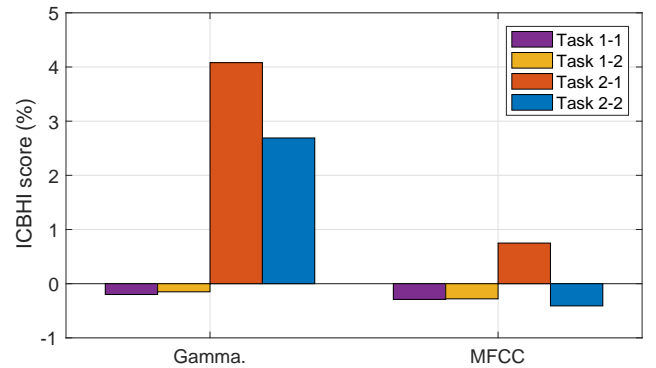


Fig. 3. Performance comparison between log-Mel and Gamma., MFCC

as shown in the Figure 2 indicate that MFCC, log-Mel, and

Gamma. performance are equal in general and much better than CQT over all Tasks. If we consider log-Mel scores as standard, Figure 3 indicates how performance difference between log-Mel and Gamma. or MFCC. It can be seen that Gamma. outperforms other spectrograms over Task 1, reports an improvement of 4% and 3.2% compared with log-Mel and MFCC, respectively. However, both Gamma. and MFCC shows little poorer performance than log-Mel in Task 2. From obtained results on spectrograms, we decide to use Gamma. for anomaly cycles detection (Task 1-1 and 1-2) and log-Mel for respiratory diseases detection (Task 2-1 and 2-2). Note that using Gamma. and log-Mel are applied for next all experiments presented below.

B. Cycle length analysis

Respiratory cycles in the ICBHI dataset have diverse lengths ranging from 0.2 s to 16.2 s with 80% of cycles being less than 5 s. It is, therefore, interesting to understand how respiratory cycle length affects classification accuracy. By using the baseline proposed in Section III-C with Gamma. spectrogram indicated in Section IV-A, we evaluated cycle length from 3 to 8 s, called standard lengths. To deal with short cycles, we duplicate them to obtain new cycles that are equal or longer than standard lengths before transforming into spectrograms. The Table III reports Task 1-1 and 1-2

TABLE III
RESPIRATORY CYCLE LENGTH ANALYSIS ON TASK 1 (%)

Task	Cyc. Len.	Spec.	Sen.	ICBHI Score
1-1, 4-category	3 s	84.20	70.92	77.56
1-1, 4-category	4 s	83.52	71.54	77.53
1-1, 4-category	5 s	84.20	73.08	78.64
1-1, 4-category	6 s	81.45	73.07	77.27
1-1, 4-category	7 s	82.56	73.54	78.05
1-1, 4-category	8 s	86.95	69.84	78.40
1-2, 2-category	3 s	84.20	81.85	83.03
1-2, 2-category	4 s	83.52	83.54	83.53
1-2, 2-category	5 s	84.20	83.69	83.95
1-2, 2-category	6 s	81.45	81.46	82.81
1-2, 2-category	7 s	82.56	84.31	83.43
1-2, 2-category	8 s	86.95	80.92	83.94

results for different cycle lengths. The best ICBHI scores are 78.64 and 83.95 for 4- and 2-category sub-tasks respectively with cycle length set to 5 s (same as the baseline's setting). Although 7 or 8-s cycle lengths also show competitive results, we choose the shorter length of 5 s for further experiments due to reducing running cost and the best results obtained.

C. Overlap/non-overlap splitting analysis

As spectrogram representation of an entire cycle or audio recoding is too long in terms of temporal dimension, they are split into smaller patches of 64×64 that is suitable for back-end deep learning models. Overlap splitting is considered to be useful to make temporal sequence continuous. This Section, therefore, evaluates if overlap splitting should be applied. As obtained results shown in Figure 4, classifying anomaly cycles in sub task 1-1 and 1-2 achieves the best core of 76.59% and 78.57% respectively with overlap patches. By

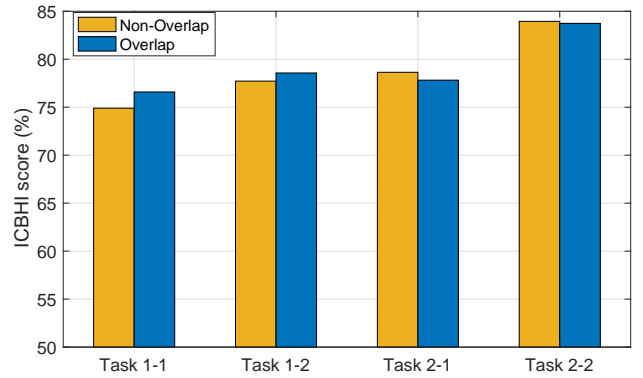


Fig. 4. Performance comparison between non-overlap and overlap splitting option on all tasks

contrast, non-overlap splitting is more effective for Task 2-1 and 2-2 with entire recordings, reports 78.64% and 83.95%, respectively.

D. Time resolution analysis

The baseline network operates on patches, with the horizontal dimension denoting the time span for each feature. Features are sequential, so the time span also sets the temporal resolution of the features. To explore, we adjust patch widths to 0.6 s, 1.2 s, 1.8 s, 2.4 s, and 3 s by setting the patch dimension to be 64×32 , 64×64 , 64×96 , 64×128 , and 64×160 , respectively, then retrain and evaluate performance of each. Results shown in Figure 5 indicate that while patch

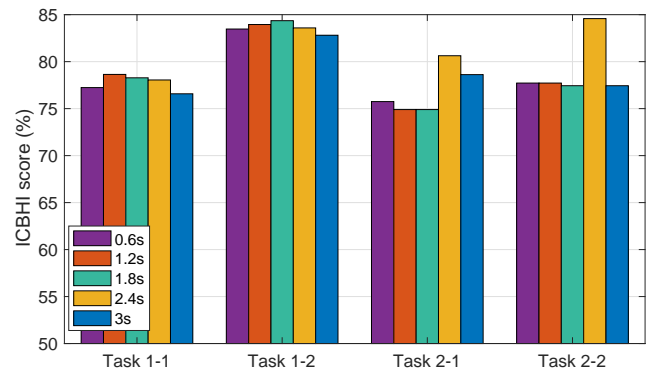


Fig. 5. Performance comparison among time resolutions on all tasks

of 64×64 (1.2 s) is the best choice with 78.64% and 83.95% for Task 1-1 and Task 1-2 respectively, Task 2-1 and 2-2 achieve the best score of 80.63% and 84.58% with patch size of 64×128 (2.4 s).

E. Data augmentation analysis

Data augmentation is useful to enforce learning ability of deep learning models that was proven in [30], [29]. In this paper, we, therefore, apply a data augmentation method, namely mixup [33], [34], [35], and evaluate if it is useful for respiratory sounds. Let consider \mathbf{X}_1 and \mathbf{X}_2 as two image patches randomly selected from the set of original image patches with their labels y_1 and y_2 , respectively, mixup

data augmentation helps to generate new image patches as Equations below,

$$\mathbf{X}_{\text{mp1}} = \mathbf{X}_1 \cdot \lambda + \mathbf{X}_2 \cdot (1 - \lambda) \quad (10)$$

$$\mathbf{X}_{\text{mp2}} = \mathbf{X}_1 \cdot (1 - \lambda) + \mathbf{X}_2 \cdot \lambda \quad (11)$$

$$\mathbf{y}_{\text{mp1}} = \mathbf{Y}_1 \cdot \lambda + \mathbf{Y}_2 \cdot (1 - \lambda) \quad (12)$$

$$\mathbf{y}_{\text{mp2}} = \mathbf{Y}_1 \cdot (1 - \lambda) + \mathbf{Y}_2 \cdot \lambda \quad (13)$$

where α is drawn from both uniform distribution or beta distribution, \mathbf{X}_{mp1} and \mathbf{X}_{mp2} are two new image patches resulted by mixing \mathbf{X}_1 and \mathbf{X}_2 with a random mixing coefficient α . After mixup, old data and generated data from mixup data augmentation are shuffled and feed into **C-DNN** baseline proposed, double batch size and consider learning time (Noting that as categories classified in Task 1-1 and 1-2 comprise of *Crackle*, *Wheeze*, *Crackle & Wheeze* and *Normal*, each of two original patches selected for mixup data augmentation is from either *Normal* or the group of anomaly cycles. However, this selection is randomly in Task 2-1 and 2-2).

By applying mixup data augmentation technique, the new labels \mathbf{y}_{mp1} and \mathbf{y}_{mp2} of the two mixup patches are no longer one-hot labels, Kullback-Leibler (KL) divergence loss [36] rather than the standard cross-entropy loss is used as shown in Equation below,

$$\text{Loss}_{KL}(\theta) = \sum_{n=1}^N \mathbf{y}_n \log\left(\frac{\mathbf{y}_n}{\hat{\mathbf{y}}_n}\right) + \frac{\lambda}{2} \|\theta\|_2^2, \quad (14)$$

where $\text{Loss}(\theta)$ is KL-loss function, θ denotes the trainable network parameters and λ denote the ℓ_2 -norm regularization coefficient, set to 0.0001, N is the batch number. \mathbf{y}_c and $\hat{\mathbf{y}}_c$ denote the ground-truth and the network output, respectively. Obtained results in Figure 6 indicates that applying mixup

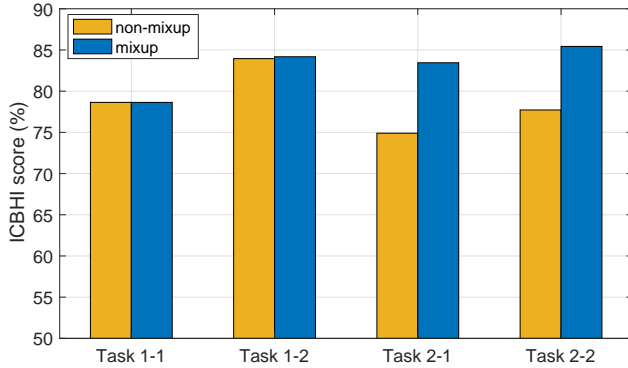


Fig. 6. Improve performance by using mixup data augmentation

data augmentation is effective to improve the classification accuracy on all tasks. Noticeably, it helps Task 2-1 and 2-2 significantly improve by 8.5% and 8.2%, respectively..

TABLE IV
DEEP LEARNING FRAMEWORK SETTING

Factors	Anomaly cycles detection	Respiratory diseases detection
Re-sample	16KHz	16KHz
Cycle duration	5s	-
Spectrogram	Gamma.	log-Mel
Patch Splitting	overlap	non-overlap
Patch size	64 × 64	64 × 128
Data augmentation	True	True
Deep learning model	C-DNN with MoE	C-DNN with MoE

V. PROPOSE ROBUST DEEP LEARNING FRAMEWORKS

From the comprehensive analysis of influencing factors in deep learning based system above, we propose two deep learning frameworks, each which is applied for either task of anomaly cycle detection or respiratory disease detection with setting shown as Table IV. As regards deep learning models, we use a same network architecture for all Tasks, namely C-DNN with MoE, which is an improvement of C-DNN baseline presented in the next Section.

A. Improve deep learning C-DNN model

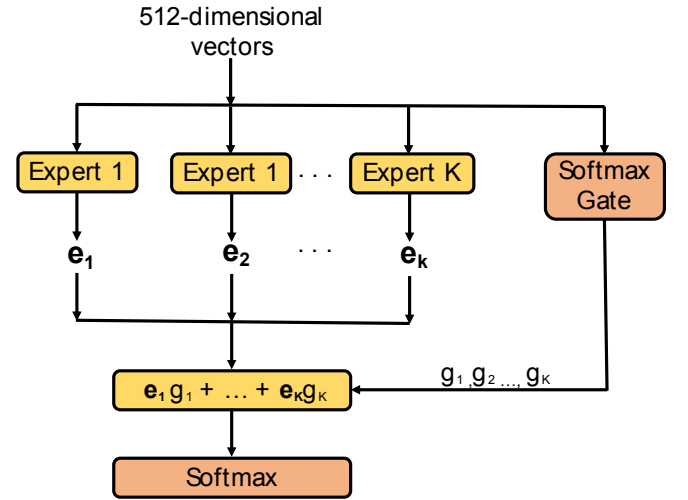


Fig. 7. MoE block architecture

Review the C-DNN baseline as shown in Table I, the first six Conv. Blocks are used to map image patch input to condensed vector features (output of the global mean pooling layer in Conv. Block 06). Thus, these vectors are classified by a fully-connected layer and a Softmax layer in the final Dense Block. Inspire that the condensed vector features extracted by global mean across channel dimension may not capture enough information, we extract more information by separately using two other pooling layers which are global max pooling and global conv. pooling. While global max pooling is widely used, the global conv. pooling proposed is an added convolutional layer with kernel size set to frequency and temporal dimensions and filter number set to channel dimension. In particular, the output shape of the tensor at the final convolutional layer in C-DNN baseline is $[n \times 8 \times 8 \times 512]$ where n is batch size and 8, 8, and 512 are frequency,

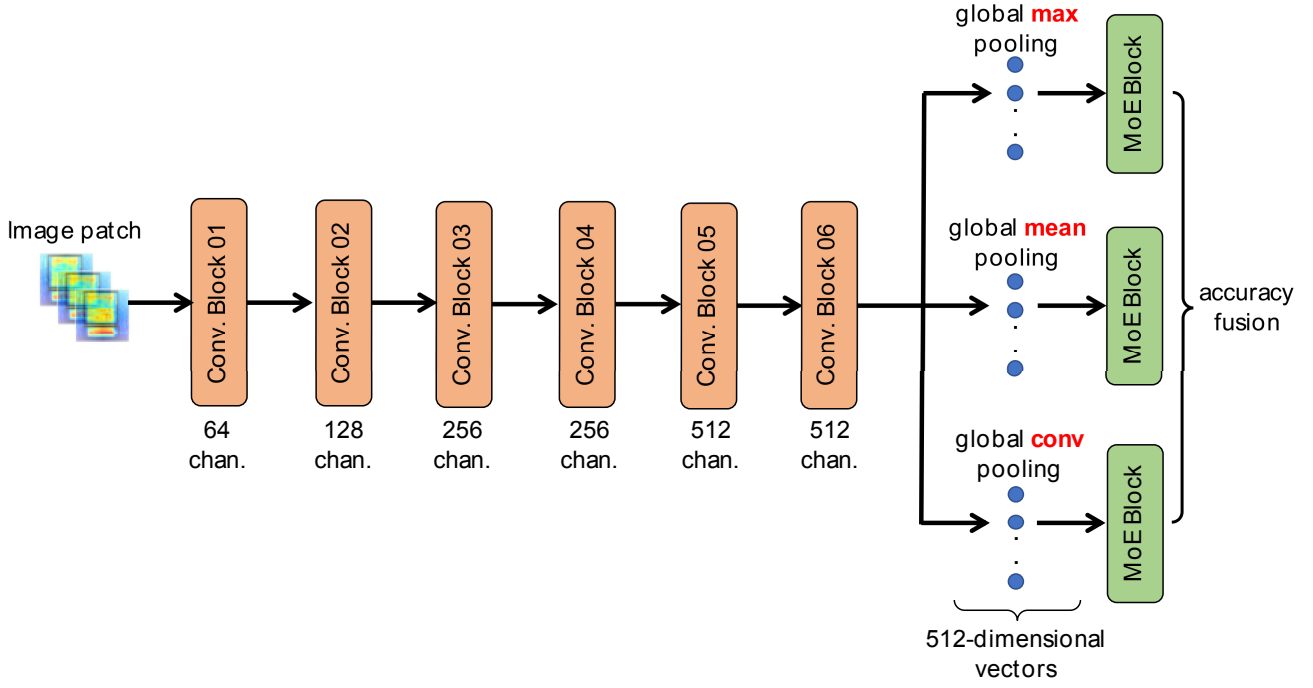


Fig. 8. Proposed deep learning model

temporal and channel dimensions, respectively. Thus, we apply a convolutional layer with kernel size of $[8 \times 8]$ and 512 filter on the tensor, thus obtain a 512-dimensional vectors. By using three types of pooling layers (global max pooling, global mean pooling, and conv. pooling), we capture as much information as possible. Each type of pooling layer extracts a 512-dimensional vector as shown in Figure 8. The second improvement is focusing on Dense Block architecture which takes the role of final classification. Particularly, we replace Dense Block by MoE block. A conventional MoE block architecture comprises many experts and incorporates a gate network to decide which expert is applied in which input region as shown in Figure 7. In our context, the 512-dimensional input vector extracted from pooling layers mentioned goes through the experts. Next the experts is gated before passing through a softmax to determine the final score. Each MoE expert comprises a fully-connected layer and a ReLu activation function. Its input dimension is 512 and its output size is the number or categories C classified. The gate network is implemented as a **Softmax Gate** – an additional fully-connected layer with softmax activation function and a gating dimension equal to the number of experts. Let $\mathbf{e}_1, \mathbf{e}_2, \dots, \mathbf{e}_K \in \mathbf{R}^C$ be the output vectors of the K experts, and g_1, g_2, \dots, g_K be the outputs of the gate network where $g_k \in \mathbf{R}, \sum_{k=1}^K g_k = 1$. The predicted output is then found as,

$$\hat{y} = \text{softmax} \left\{ \sum_{k=1}^K \mathbf{e}_k g_k \right\}. \quad (15)$$

B. Experimental setting and accuracy fusion

As setting mentioned in Table IV for proposed deep learning frameworks, mixup data augmentation is used, thus

make label not shape of one-hot coding. Therefore, Kullback-Leibler (KL) divergence loss [36] mentioned in Section IV-E and Equation (14) is used to train deep learning models proposed (C-DNN with MoE). We use TensorFlow framework to build the model and set learning rate=0.0001, epoch num=100, batch size=100, initial trainable parameters by Normal Distribution with mean=0 and standard deviation=0.1.

As using three types of pooling layers, we apply *mean-fusion* method to fuse posterior probability obtained. Let us consider $\mathbf{P}^{m,n} = (\mathbf{p}_1^{m,n}, \mathbf{p}_2^{m,n}, \dots, \mathbf{p}_C^{m,n})$, with C being the category number, the n^{th} out of N patches fed into learning model, and the m^{th} out of 3 types of pooling layers to be the probability of a test sound instance. The mean classification probability is then denoted as $\bar{p} = (\bar{p}_1, \bar{p}_2, \dots, \bar{p}_C)$ where,

$$\bar{p}_c = \frac{1}{3 \cdot N} \sum_{m=1}^3 \sum_{n=1}^N \mathbf{p}_c^{m,n} \quad \text{for } 1 \leq n \leq N, 1 \leq m \leq 3 \quad (16)$$

and similarly the predicted label is determined as in Equation (9).

C. Performance compared to the state of the art

From the experimental analysis results, we propose separate network configurations for ICBHI challenge Tasks 1 and 2, although both share the same deep learning model (C-DNN+MoE).

Table V (top) compares the proposed Task 1 system against the state of the art, demonstrating the highest accuracy of 0.81 and 0.86 for the 4-category and 2-category subtasks, respectively. Task 2 results (Table V, bottom) reveal

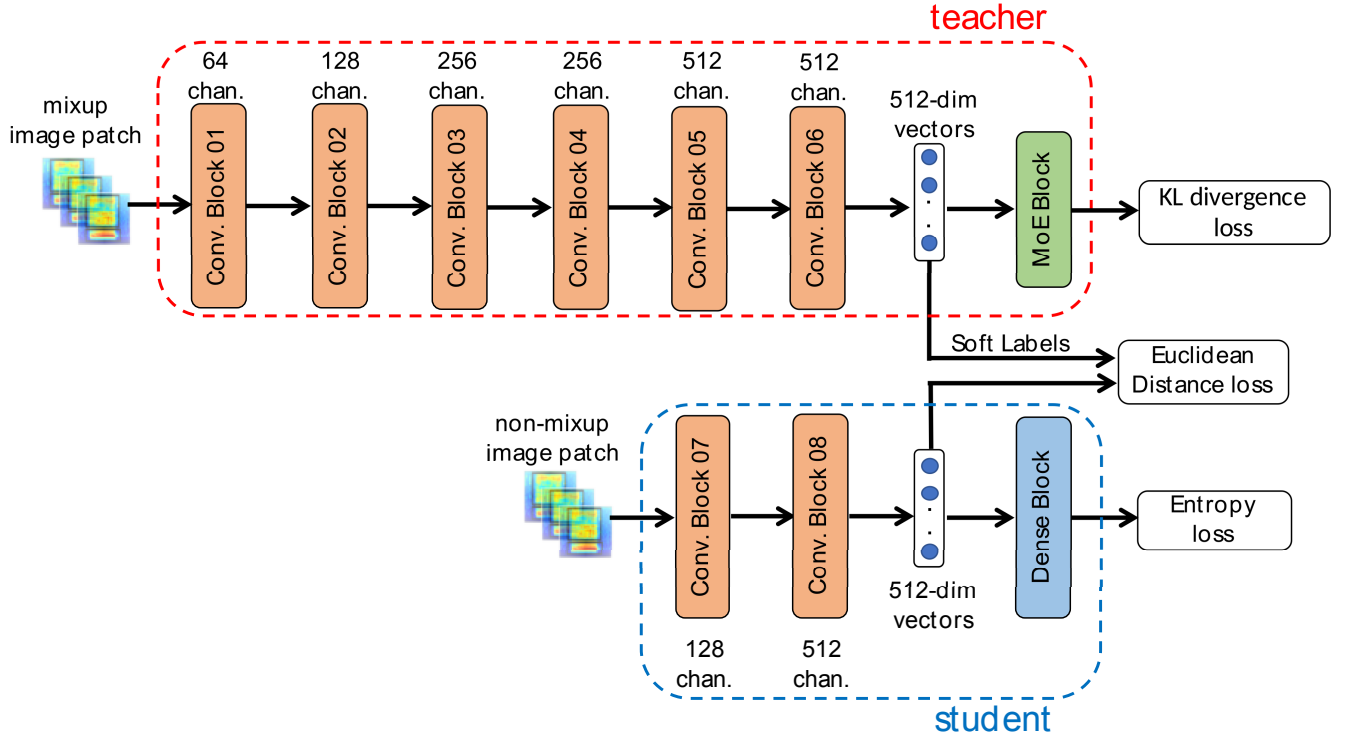


Fig. 9. Teacher-Student scheme architecture

TABLE V
COMPARISON AGAINST STATE-OF-THE-ART SYSTEMS

Task	Method	train/test	Spec.	Sen.	ICBHI Score
1-1, 4-class	Boosted Tree [8]	60/40	0.78	0.21	0.49
1-1, 4-class	CNN-RNN [19]	80/20	-	-	0.66
1-1, 4-class	CNN [21]	80/20	0.77	0.45	0.61
1-1, 4-class	MNRNN [24]	five folds	0.74	0.56	0.65
1-1, 4-class	LSTM [22]	80/20	0.85	0.62	0.74
1-1, 4-class	Our system	five folds	0.87	0.74	0.81
1-2, 2-class	LSTM [22]	80/20	-	-	0.81
1-2, 2-class	CNN [18]	75/25	-	-	0.82
1-2, 2-class	Our system	five folds	0.86	0.85	0.86
2-1, 3-class	CNN [21]	80/20	0.76	0.89	0.83
2-1, 3-class	LSTM [22]	80/20	0.82	0.98	0.90
2-1, 3-class	Our system	five folds	0.86	0.95	0.91
2-2, 2-class	CNN-RNN [19]	60/40	-	-	0.71
2-2, 2-class	CNN [21]	80/20	0.78	0.97	0.88
2-2, 2-class	RUSBoost [6]	50/50	0.93	0.86	0.90
2-2, 2-class	LSTM [22]	80/20	0.82	0.99	0.91
2-2, 2-class	Our system	five folds	0.86	0.98	0.92

an accuracy of 0.91 and 0.90 for the 3-category and 2-category subtasks respectively. These results indicate that our proposed deep learning frameworks outperform the state-of-the-art methods. However, the comparison may be not 100% exact due to different proportion splitting over dataset.

VI. STUDENT-TEACHER SCHEME TO REDUCE MODEL SIZE FOR RESPIRATORY DISEASES DETECTION

A. Student-Teacher scheme

Inspiration from effectively applying Teacher-Student scheme on sound scenes and sound events [37], [38], we apply this technique on Task 2 to deal with the trade-off between model size and performance. The proposed

Teacher-Student scheme as described in Figure 9 comprises of two networks, namely Teacher (the upper) and Student (the lower), respectively. Teacher network reuses the C-DNN+MoE architecture introduced in Section V-A with only using global mean pooling. As regards the Student network architecture, it comprises of two Conv. Block 07, 08, and a Dense Block with configuration as denoted in Table VI. Note that Conv. Blocks used in Student network do not apply Batchnorm and Dropout layers. To operate the scheme, training Teacher-Student scheme is separated into two phases. The Teacher is firstly trained, thus extract the output of global mean pooling layer. The extracted features, likely 512-dimensional vectors, are referred as to soft labels that will be used to train Student network. Since we obtain the soft labels from the Teacher network, we train the Student network by combining two loss functions. The first loss function used Euclidean distance aims to minimize difference between soft labels and 512-dimensional vectors extracted from the output of global mean pooling layer on the Student network. Meanwhile, the second Cross-Entropy loss function is used for classification of three groups of respiratory diseases. Eventually, the final loss is described below,

$$Loss(\theta) = Loss_{Entropy}(\theta) + \gamma \cdot Loss_{Euclidean}(\theta) \quad (17)$$

where $Loss_{Entropy}$ and $Loss_{Euclidean}$ are the Cross-Entropy and Euclidean distance losses respectively. Hyper-parameter γ is experimentally set to 1/2. θ is total trainable parameters.

TABLE VI
STUDENT NETWORK ARCHITECTURE

Architecture	layers	Output
Conv. Block 07	Input layer (image patch)	64×128
Conv. Block 08	Cv [3×3] - Relu - Ap [4×4]	16×32×128
Dense Block	Cv [3×3] - Relu - Gap	512
	Fl - Softmax layer	3

B. Experimental results

TABLE VII
PERFORMANCE COMPARISON AMONG STUDENT NETWORK ONLY,
TEACH NETWORK ONLY, AND TEACHER-STUDENT SCHEME

Task	Method	Spec.	Sen.	ICBHI Score
2-1, 3-class	Teacher	0.86	0.95	0.91
2-1, 3-class	Student only	0.43	0.94	0.68
2-1, 3-class	Student with soft labels	0.86	0.90	0.88
2-2, 2-class	Teacher	0.86	0.98	0.92
2-2, 2-class	Student only	0.43	0.99	0.71
2-2, 2-class	Student with soft labels	0.86	0.96	0.91

From results obtained as in Table VII, Student network trained with soft labels from Teacher network achieves 0.88 and 0.91 on Task 2-1 and 2-2, respectively. Although Student network cannot reach the scores of Teacher network with 0.91 and 0.92 on Task 2-1 and 2-2 respectively, Student network helps to significantly reduce the size of reference model without reducing performance too much. Look at results on Student network without soft labels from Teacher, the performance significantly reduces to 0.68 and 0.71 for Task 2-1 and 2-2, respectively. As a result, apply Teacher-Student scheme helps to achieve a Student network with lower parameter of 7296, compared with 30912 trainable parameters in Teacher network, which is effectively used for detection processes in low-parameter required systems.

VII. CONCLUSION

This paper has presented an exploration of deep learning models for detecting respiratory disease from auditory recordings. By conducting intensive experiments over the ICBHI dataset, we propose deep learning frameworks for four challenge tasks of respiratory sound classification. The proposed systems are shown to outperform the state of the art on all tasks. Furthermore, effectively applying Teacher-Student scheme helps to significantly reduce model size used for reference process but still achieves high performance. Obtained experimental results validate application of deep learning for early diagnosis of respiratory disease.

REFERENCES

- [1] World Health Organization, "The global impact of respiratory diseases (second edition)," 2017.
- [2] Hüseyin Polat and İnan Güler, "A simple computer-based measurement and analysis system of pulmonary auscultation sounds," *Journal of medical systems*, vol. 28, no. 6, pp. 665–672, 2004.
- [3] R. J. Riella, P. Nohama, R. F. Borges, and A. L. Stelle, "Automatic wheezing recognition in recorded lung sounds," in *Proc. EMBC*, Sep. 2003, vol. 3, pp. 2535–2538.
- [4] Sandra Reichert, Raymond Gass, Christian Brandt, and Emmanuel Andrés, "Analysis of respiratory sounds: state of the art," *Clinical medicine. Circulatory, respiratory and pulmonary medicine*, vol. 2, pp. CCRPM-S530, 2008.

- [5] Takanori Okubo, Naoki Nakamura, Masaru Yamashita, and Shoichi Matsunaga, "Classification of healthy subjects and patients with pulmonary emphysema using continuous respiratory sounds," in *2014 36th Annual International Conference of the IEEE Engineering in Medicine and Biology Society*. IEEE, 2014, pp. 70–73.
- [6] Xuen Hoong Kok, Syed Anas Imtiaz, and Esther Rodriguez-Villegas, "A novel method for automatic identification of respiratory disease from acoustic recordings," in *2019 41st Annual International Conference of the IEEE Engineering in Medicine and Biology Society (EMBC)*. IEEE, 2019, pp. 2589–2592.
- [7] Morten Grønnesby, Juan Carlos Aviles Solis, Einar Holsbø, Hasse Melbye, and Lars Ailo Bongo, "Feature extraction for machine learning based crackle detection in lung sounds from a health survey," *arXiv preprint arXiv:1706.00005*, 2017.
- [8] Gaëtan Chambres, Pierre Hanna, and Myriam Desainte-Catherine, "Automatic detection of patient with respiratory diseases using lung sound analysis," in *Proc. CBMI*, 2018, pp. 1–6.
- [9] Luis Mendes, Ioannis M Vogiatzis, Eleni Perantoni, Evangelos Kaimakamis, Ioanna Chouvarda, Nicos Maglaveras, Jorge Henriques, Paulo Carvalho, and Rui Pedro Paiva, "Detection of crackle events using a multi-feature approach," in *2016 38th Annual International Conference of the IEEE Engineering in Medicine and Biology Society (EMBC)*. IEEE, 2016, pp. 3679–3683.
- [10] Shreyasi Datta, Anirban Dutta Choudhury, Parijat Deshpande, Sakyajit Bhattacharya, and Arpan Pal, "Automated lung sound analysis for detecting pulmonary abnormalities," in *2017 39th Annual International Conference of the IEEE Engineering in Medicine and Biology Society (Embc)*. IEEE, 2017, pp. 4594–4598.
- [11] David N Reshef, Yakir A Reshef, Hilary K Finucane, Sharon R Grossman, Gilean McVean, Peter J Turnbaugh, Eric S Lander, Michael Mitzenmacher, and Pardis C Sabeti, "Detecting novel associations in large data sets," *science*, vol. 334, no. 6062, pp. 1518–1524, 2011.
- [12] Nandini Sengupta, Md Sahidullah, and Goutam Saha, "Lung sound classification using local binary pattern," *arXiv preprint arXiv:1710.01703*, 2017.
- [13] Dinko Oletic, Marko Matijascic, Vedran Bilas, and Michele Magno, "Hidden markov model-based asthmatic wheeze recognition algorithm leveraging the parallel ultra-low-power processor (pulp)," in *2019 IEEE Sensors Applications Symposium*, 2019, pp. 1–6.
- [14] Gorkem Serbes, Sezer Ulukaya, and Yasemin P Kahya, "An automated lung sound preprocessing and classification system based on spectral analysis methods," in *Precision Medicine Powered by pHealth and Connected Health*, 2018, pp. 45–49.
- [15] Haomin Zhang, Ian McLoughlin, and Yan Song, "Robust sound event recognition using convolutional neural networks," in *Proc. ICASSP*, Apr. 2015, number 2635, pp. 559–563.
- [16] Ian McLoughlin, Yan Song, Lam Dam Pham, Huy Pham, Palaniappan Ramaswamy, and Lang Yue, "Early detection of continuous and partial audio events using CNN," in *Proc. INTERSPEECH*, 2018.
- [17] Lukui Shi, Kang Du, Chaozong Zhang, Hongqi Ma, and Wenjie Yan, "Lung sound recognition algorithm based on vggish-bigru," *IEEE Access*, vol. 7, pp. 139438–139449, 2019.
- [18] Renyu Liu, Shengsheng Cai, Kexin Zhang, and Nan Hu, "Detection of adventitious respiratory sounds based on convolutional neural network," in *2019 International Conference on Intelligent Informatics and Biomedical Sciences (ICIIBMS)*. IEEE, 2019, pp. 298–303.
- [19] J Acharya and A Basu, "Deep neural network for respiratory sound classification in wearable devices enabled by patient specific model tuning," *IEEE transactions on biomedical circuits and systems*, 2020.
- [20] Murat Aykanat, Özkan Kılıç, Bahar Kurt, and Sevgi Saryal, "Classification of lung sounds using convolutional neural networks," *EURASIP Journal on Image and Video Processing*, vol. 2017, no. 1, pp. 65, 2017.
- [21] Diego Perna, "Convolutional neural networks learning from respiratory data," in *Proc. BIBM*, 2018, pp. 2109–2113.
- [22] Diego Perna and Andrea Tagarelli, "Deep auscultation: Predicting respiratory anomalies and diseases via recurrent neural networks," in *Proc. CBMS*, 2019, pp. 50–55.
- [23] Elmar Messner, Melanie Fediuk, Paul Swatek, Stefan Scheidl, Freyja-Maria Smolle-Jüttner, Horst Olschewski, and Franz Pernkopf, "Crackle and breathing phase detection in lung sounds with deep bidirectional gated recurrent neural networks," in *Proc. EMBC*, 2018, pp. 356–359.
- [24] Kirill Kochetov, Evgeny Putin, Maksim Balashov, Andrey Filchenkov, and Anatoly Shalyto, "Noise masking recurrent neural network for

- respiratory sound classification,” in *International Conference on Artificial Neural Networks*, 2018, pp. 208–217.
- [25] K. Minami, H. Lu, H. Kim, S. Mabu, Y. Hirano, and S. Kido, “Automatic classification of large-scale respiratory sound dataset based on convolutional neural network,” in *2019 19th International Conference on Control, Automation and Systems (ICCAS)*, 2019, pp. 804–807.
 - [26] Hai Chen, Xiaochen Yuan, Zhiyuan Pei, Mianjie Li, and Jianqing Li, “Triple-classification of respiratory sounds using optimized s-transform and deep residual networks,” *IEEE Access*, vol. 7, pp. 32845–32852, 2019.
 - [27] BM Rocha, D Filios, L Mendes, Vogiatzis, et al., “A respiratory sound database for the development of automated classification,” in *Precision Medicine Powered by pHealth and Connected Health*, pp. 33–37. 2018.
 - [28] Diederik P Kingma and Jimmy Ba, “Adam: A method for stochastic optimization,” *arXiv preprint arXiv:1412.6980*, 2014.
 - [29] Lam Pham, Ian McLoughlin, Huy Phan, and Ramaswamy Palaniappan, “A robust framework for acoustic scene classification,” in *Proc. INTERSPEECH*, 09 2019, pp. 3634–3638.
 - [30] Lam Pham, Ian McLoughlin, Huy Phan, Ramaswamy Palaniappan, and Yue Lang, “Bag-of-features models based on C-DNN network for acoustic scene classification,” in *Proc. AES*, 2019.
 - [31] McFee, Brian, Raffel Colin, Liang Dawen, Daniel. PW.Ellis, McVicar Matt, Battenberg Eric, and Nieto Oriol, “librosa: Audio and music signal analysis in python,” in *Proceedings of The 14th Python in Science Conference*, 2015, pp. 18–25.
 - [32] D P W (2009) Ellis, “Gammatone-like spectrogram,” 2009.
 - [33] Kele Xu, Dawei Feng, Haibo Mi, Boqing Zhu, Dezhi Wang, Lilun Zhang, Hengxing Cai, and Shuwen Liu, “Mixup-based acoustic scene classification using multi-channel convolutional neural network,” in *Pacific Rim Conference on Multimedia*, 2018, pp. 14–23.
 - [34] Yuji Tokozume, Yoshitaka Ushiku, and Tatsuya Harada, “Learning from between-class examples for deep sound recognition,” *arXiv preprint arXiv:1711.10282*, 2017.
 - [35] Hongyi Zhang, Moustapha Cisse, Yann N Dauphin, and David Lopez-Paz, “mixup: Beyond empirical risk minimization,” *arXiv preprint arXiv:1710.09412*, 2017.
 - [36] Solomon Kullback and Richard A Leibler, “On information and sufficiency,” *The annals of mathematical statistics*, vol. 22, no. 1, pp. 79–86, 1951.
 - [37] Hee-Soo Heo, Jee-weon Jung, Hye-jin Shim, and Ha-Jin Yu, “Acoustic scene classification using teacher-student learning with soft-labels,” *arXiv preprint arXiv:1904.10135*, 2019.
 - [38] Liang Gao, Haibo Mi, Boqing Zhu, Dawei Feng, Yicong Li, and Yuxing Peng, “An adversarial feature distillation method for audio classification,” *IEEE Access*, vol. 7, pp. 105319–105330, 2019.